



AFRL-RY-HS-TR-2010-0038

DEVELOPMENT OF RF SENSOR BASED ON TWO CELL SQUID

Ming He and Alexey Ustinov

**University of Karlsruhe
Physikalisches Institut**

**APRIL 2010
Interim Report**

Approved for public release; distribution unlimited.

See additional restrictions described on inside pages

STINFO COPY

**AIR FORCE RESEARCH LABORATORY
SENSORS DIRECTORATE
HANSCom AIR FORCE BASE, MA 01731-2909
AIR FORCE MATERIEL COMMAND
UNITED STATES AIR FORCE**

NOTICE AND SIGNATURE PAGE

Using Government drawings, specifications, or other data included in this document for any purpose other than Government procurement does not in any way obligate the U.S. Government. The fact that the Government formulated or supplied the drawings, specifications, or other data does not license the holder or any other person or corporation; or convey any rights or permission to manufacture, use, or sell any patented invention that may relate to them.

This report was cleared for public release by the Electronics Systems Center Public Affairs Office (PAO) for the Air Force Research Lab Oratory Electro Magnetics Technology Division and is available to the general public, including foreign nationals.

Copies may be obtained from the Defense Technical Information Center (DTIC)
(<http://www.dtic.mil>).

AFRL-RY-HS-TR-2010-0038 HAS BEEN REVIEWED AND IS APPROVED FOR
PUBLICATION IN ACCORDANCE WITH THE ASSIGNED DISTRIBUTION STATEMENT.

*//signature//

STANFORD P. YUKON
Senior Physicist
Electromagnetic Scattering Branch

//signature//

BERTUS WEIJERS
Branch Chief
Electromagnetic Scattering Branch

//signature//

ROBERT V. McGAHAN
Technical Communication Advisor
Electromagnetics Technology Division

This report is published in the interest of scientific and technical information exchange, and its publication does not constitute the Government's approval or disapproval of its ideas or findings.

*Disseminated copies will show “//signature//” stamped or typed above the signature blocks.

REPORT DOCUMENTATION PAGE				Form Approved OMB No. 0704-0188	
<p>The public reporting burden for this collection of information is estimated to average 1 hour per response, including the time for reviewing instructions, searching existing data sources, gathering and maintaining the data needed, and completing and reviewing the collection of information. Send comments regarding this burden estimate or any other aspect of this collection of information, including suggestions for reducing this burden, to Department of Defense, Washington Headquarters Services, Directorate for Information Operations and Reports (0704-0188), 1215 Jefferson Davis Highway, Suite 1204, Arlington, VA 22202-4302. Respondents should be aware that notwithstanding any other provision of law, no person shall be subject to any penalty for failing to comply with a collection of information if it does not display a currently valid OMB control number. PLEASE DO NOT RETURN YOUR FORM TO THE ABOVE ADDRESS.</p>					
1. REPORT DATE (DD-MM-YY) April 2010		2. REPORT TYPE Interim		3. DATES COVERED (From - To) 01 January 2009 – 31 December 2009	
4. TITLE AND SUBTITLE DEVELOPMENT OF RF SENSOR BASED ON TWO CELL SQUID				5a. CONTRACT NUMBER FA8655-09-1-3097	
				5b. GRANT NUMBER	
				5c. PROGRAM ELEMENT NUMBER 612304	
6. AUTHOR(S) Ming He and Alexey Ustinov				5d. PROJECT NUMBER 2304	
				5e. TASK NUMBER HE	
				5f. WORK UNIT NUMBER 2304HE05	
7. PERFORMING ORGANIZATION NAME(S) AND ADDRESS(ES) University of Karlsruhe Physikalisches Institut Germany				8. PERFORMING ORGANIZATION REPORT NUMBER AFRL-RY-HS-TR-2010-0038	
9. SPONSORING/MONITORING AGENCY NAME(S) AND ADDRESS(ES) Air Force Research Laboratory Sensors Directorate Hanscom Air Force Base, MA 01731-2909 Air Force Materiel Command United States Air Force				10. SPONSORING/MONITORING AGENCY ACRONYM(S) AFRL/RHYE	
				11. SPONSORING/MONITORING AGENCY REPORT NUMBER(S) AFRL-RY-HS-TR-2010-0038	
12. DISTRIBUTION/AVAILABILITY STATEMENT Approved for public release; distribution unlimited.					
13. SUPPLEMENTARY NOTES PAO Case Number: 66ABW-2010-1169; cleared 30 September 2010. This report contains the results from research and development sponsored and/or monitored by the Sensors Directorate at the Air Force Research Laboratory (AFRL) Hanscom Research Site, MA. The AFRL Hanscom Research Site was closed in 2012 as part of the Base Realignment and Closure Commission (BRAC) process. This report is the best available copy at time of publication. Report contains color.					
14. ABSTRACT Proposed to develop and investigate a sensitive microwave sensor based on a two-cell SQUID by imitating the operational principle of the fly's ears. The fly ormia shows astonishing localization ability with its tiny hearing organ. We show first measurement results based on several available Josephson junction (JJ) circuits. We investigated the current-voltage characteristics as a function of external magnetic field. We have also developed a new experimental setup for applying microwave signals with controllable phase shift and observed the response of the SQUID circuits to small variations of the phase and/or amplitude of two microwave signals coupled off-chip. We find that the dc voltage of the studied two-cell SQUID varied by 0.02 μ V under the change of the phase difference of the microwave radiation signal by 1°. Furthermore, we designed new specially tailored SQUID circuits dedicated for measurements of the microwave phase difference between two incoming signals.					
15. SUBJECT TERMS single cell SQUIDS, superconducting quantum interference devices, perturbation solution, SQIF, superconducting quantum interference filters					
16. SECURITY CLASSIFICATION OF:			17. LIMITATION OF ABSTRACT: SAR	18. NUMBER OF PAGES 16	19a. NAME OF RESPONSIBLE PERSON (Monitor) Stanford P. Yukon 19b. TELEPHONE NUMBER (Include Area Code) N/A
a. REPORT Unclassified	b. ABSTRACT Unclassified	c. THIS PAGE Unclassified			

TABLE OF CONTENTS	Page
Abstract	1
1. Introduction	1
2. Experimental Setup and Results	1
2.1 Experiment Setup	2
2.2 Experimental Results and Analysis	3
2.21 One Josephon junction circuit	3
2.22 One-cell SQUID circuit with two JJs	4
2.23 Two-Cell SQUID with Seven JJs	6
3. New Design	9
4. Conclusion	10
References	10

LIST OF FIGURES

- Figure 1. The Schematic view of the electronic setup of the measurements.
- Figure 2. (a) Optical image of one JJ circuit
(b) The sketch of the circuit and the coupling of two external microwave signals. The JJ is indicated by cross.
- Figure 3. (a) The current-voltage characteristics of the single-JJ circuit taken at fixed microwave power for several different values of the phase difference. The frequency of the microwave radiation is 20GHz.
(b) The current amplitude of the first Shapiro step versus the phase difference β .
- Figure 4. (a) The optical image of the one-cell SQUID circuit with two JJs.
(b) The sketch of the one-cell SQUID circuit. The JJs are indicated by the cross.
- Figure 5. (a) The current-voltage characteristics of the one-cell SQUID for several different values of the phase difference β . The frequency of the microwave radiation is 20GHz.
(b) The dependence of the height of the first Shapiro step of the one-cell SQUID on the phase difference of two microwave radiation signals.
- Figure 6. The dependence of the critical currents of the one-cell SQUID on the externally applied dc magnetic fluxes.
- Figure 7. The current-voltage characteristics of on-cell SQUID under a microwave radiation. Different curves represent the current-voltage characteristics at different amplitudes of external dc magnetic fluxes.
- Figure 8. (a) Optional image of the two-cell SQUID with seven JJs. The dimension of the holes is $18 \times 18 \mu\text{m}^2$. The distance between the two holes is $90 \mu\text{m}$.
(b) The sketch of the two-cell SQUID circuit. The sever JJs are indicated by crosses.
- Figure 9. The current-voltage characteristics of two-cell SQUOD with (black line) and without (red line) microwave radiation. The frequency of the microwave radiation is 19.22GHz.
- Figure 10. The dependence of the critical currents of the two-cell SQUOD on the externally applied DC magnetic flux.
- Figure 11. The current-voltage characteristics of the two-cell SQUID irradiated by a microwave signal. Different curves represent the current-voltage characteristics at different amplitudes of external DC magnetic fluxes. The frequency of the microwave radiation signal is 19.22GHz.
- Figure 12. The current-voltage characteristics of the two-cell SQUID under the radiation of two microwave signals for different values of the phase difference β . The frequency of the microwave radiation is 19.22GHz.
- Figure 13. (a) The sketch of how to measure the voltage variations versus the phase difference.
(b) The voltage variations versus the phase difference. The frequency of the microwave radiation is 19.22GHz.
- Figure 14. Schematic diagram of the relationship of the incoming angle θ and the phase difference β .
- Figure 15. (a) The sketch and (b) the layout of the two-cell SQUID circuit.

ABSTRACT

In this project, we proposed to develop and investigate a sensitive microwave sensor based on a two-cell SQUID by imitating the operational principle of the fly's ears. The fly ormia shows astonishing localization ability with its tiny hearing organ. In this report, we show first measurement results based on several available Josephson junction (JJ) circuits. We investigated the current-voltage characteristics as a function of external magnetic field. We have also developed a new experimental setup for applying microwave signals with controllable phase shift and observed the response of the SQUID circuits to small variations of the phase and/or amplitude of two microwave signals coupled off-chip. We find that the dc voltage of the studied two-cell SQUID varied by $0.02\text{ }\mu\text{V}$ under the change of the phase difference of the microwave radiation signal by 1° . Furthermore, we designed new specially tailored SQUID circuits dedicated for measurements of the microwave phase difference between two incoming signals. The designed circuits have been submitted for fabrication at Hypres Inc.

1. Introduction

A small yellow tachinid fly ormia is able to sense a small signal phase difference by using its evolutionally developed hearing system to couple the two tympani by a stiff membrane, so that the coupled tympani have two frequency sensitive modes. The membrane antisymmetric mode is dominant and yields a signal that is large enough to establish the direction of the acoustic source. The directional acuity in the hearing of the tachinid fly ormia allows to determine the direction of incoming sound to the $\sim 2.5^\circ$ accuracy. [1, 2]

Inspired by the hearing ability of the fly, we proposed to build a directional microwave sensor based on the operational principle of the fly's ears. We would like to use for that two LC resonant modes of a two-cell SQUID. Two possible operation modes for the two-cell SQUID are (i) operating it in a passive way without dc bias currents and (ii) with dc currents biasing the SQUID in a finite voltage state. We have searched for the response sensitivity of the SQUID to small variations of the phase and/or amplitude of the microwave signals that are coupled to the two SQUID cells. Since the variation of the phase and/or the amplitude of the microwave signals between the two cells of the SQUID is a function of the angle of the incoming microwave, this device can be used to detect the incident angle of the microwave signal.

2. Experimental Setup and Results

We started from experiments on a Josephson junction circuit and then single and double cell SQUID circuits, which were previously developed for different type of experiments. We investigated the current-voltage characteristics modulated with

external magnetic field and the response sensitivity to variations of the phase of the microwave signal coupled to the circuits.

2.1 Experiment Setup

A standard experimental setup for measurements at liquid helium temperature was employed for testing the samples and evaluation of their parameters at $T = 4.2$ K. The sample, mounted on a dip-stick using a suitable holder, is remaining in the vapor above the surface of liquid helium. This allows us to control the temperature of the sample in the range from 4.2 K to 6.5 K. The temperature of the sample was close increased by lifting the sample to different positions that are slightly above the liquid helium surface.

The sample is ultrasonically bonded to a sample holder through aluminum wires with a diameter of $25\mu\text{m}$. The symmetric low-pass RC filters (with ~ 15 dB cut-off frequency at ~ 1 kHz) on the sample holder shield the sample from external high-frequency electromagnetic interference. The sample is connected to the external analog electronics via twisted wires. To exclude the line resistances from the measurement, we use a standard four-point measurement technique. The shielding of the system from external dc magnetic fields is achieved through a cryoperm cylinder enclosing the bottom part of the dip-stick. A coil, placed below the sample holder, allows applying a magnetic field perpendicular to the plane of the sample. The microwave radiation was provided through two coaxial cables each ending with a small closed loop. Figure 1 shows the schematic view of the electronic setup that was employed for the measurements.

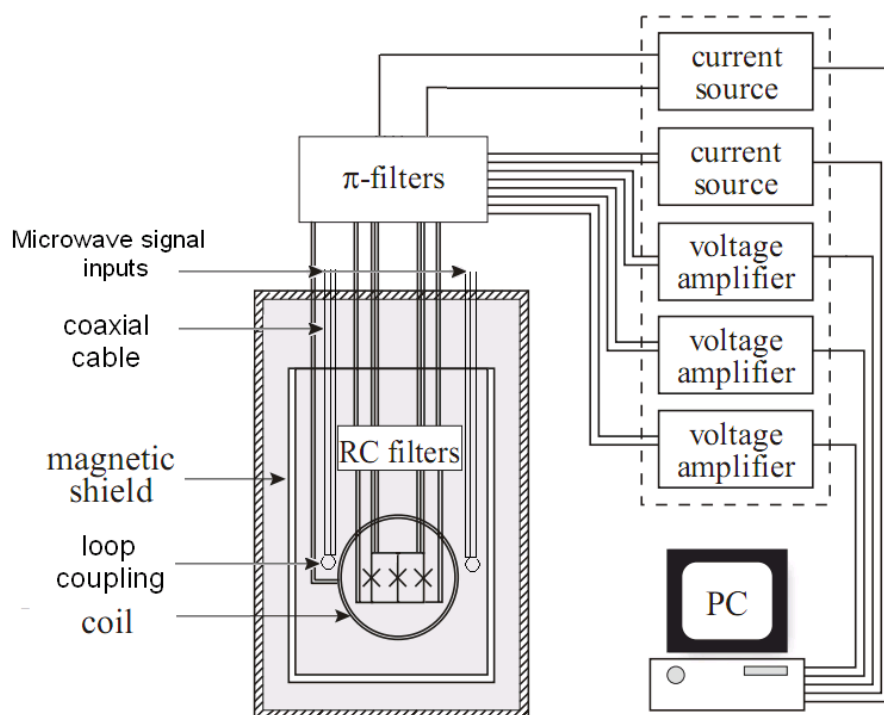


Figure 1. The schematic view of the electronic setup of the measurements.

2.2 Experimental Results and Analysis

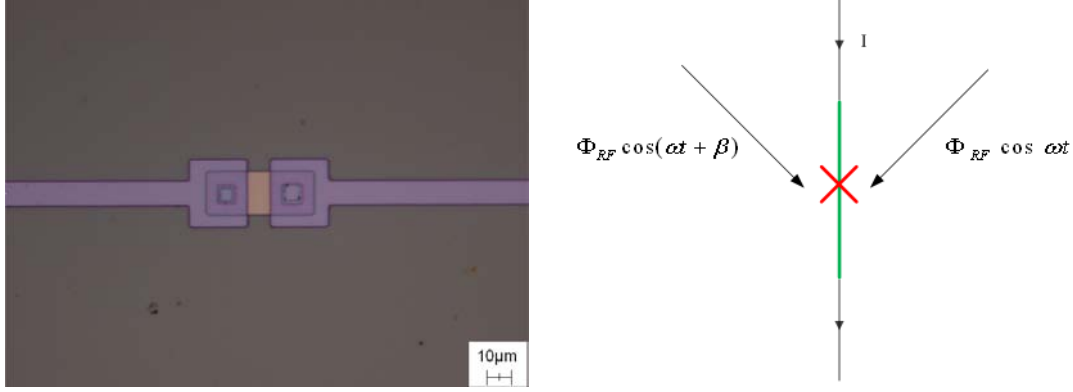


Figure 2. (a) Optical image of one JJ circuit.

(b) The sketch of the circuit and the coupling of two external microwave signals. The JJ is indicated by cross.

The investigated Josephson junction circuits are constituted by the lumped Nb/Al-AlO_x/Nb tunnel JJs. Niobium (Nb) is used as superconducting material with critical temperature $T_c = 9.2$ K. The insulating barrier is made of aluminum oxide (AlO_x).

2.2.1 One Josephson junction circuit

Figures 2(a) and 2(b) show the optical image and the sketch of the single-JJ circuit, respectively. The dimension of the JJ is $5 \times 5 \mu\text{m}^2$. The JJ is indicated by the cross in figure 2(b). Two microwave radiation signals with the phase difference β are coupled to the JJ by the two loops. In Figure 2(b), ω is the angular frequency of the microwave radiation and Φ_{RF} denotes the amplitude of the microwave radiation signal.

Generally, in order to observe large-amplitude Shapiro steps, the characteristic frequency of the junction $f_c = I_c R_n / \Phi_0$ should be close to the frequency f_{RF} of the microwave radiation signal. As the characteristic frequency of JJ can be adjusted by the variations of the critical current of the JJ, we figured out that the optimum results can be achieved by controlling the temperature of the sample. As the temperature change also affects the damping, data presented below refer to the overdamped junction behavior.

Figure 3(a) illustrates the current-voltage characteristics of the one-JJ circuit for several different values of phase difference β . The dashed curve marked with triangles denotes the current-voltage characteristics without external microwave radiation. It shows that the critical current $I_c = 20 \mu\text{A}$ and the normal resistance $R_n = 2.4 \Omega$, which results in the characteristic frequency of $f_c \sim 23$ GHz. From this figure, we can observe the maximum height of the first Shapiro step at $\beta = 0^\circ$ and the minimum height of the first Shapiro step at $\beta = 180^\circ$. As shown in Figure 3(b), with the increasing of the phase difference, the height of the first Shapiro step varies approximately proportionally to $|\cos(\beta/2)|$. We also investigated the current-voltage

characteristics modulated with externally applied dc magnetic fluxes. However, only small changes of the characteristics of the Shapiro steps were observed.

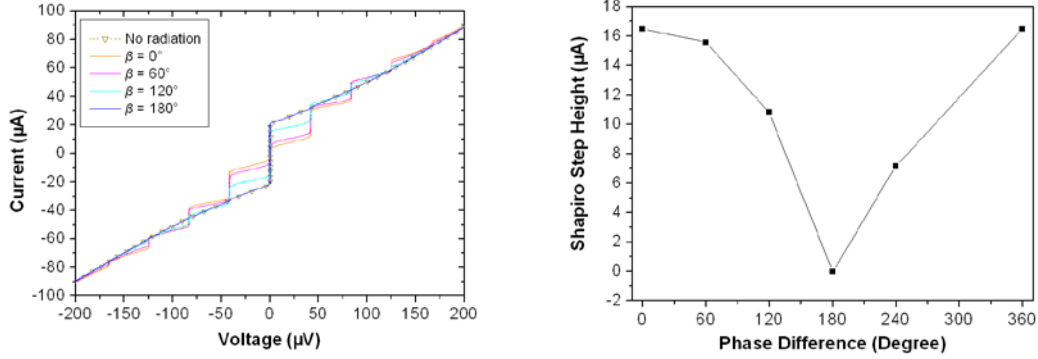


Figure 3. (a) The current-voltage characteristics of the single-JJ circuit taken at fixed microwave power for several different values of the phase difference β . The frequency of the microwave radiation is 20 GHz.

(b) The current amplitude of the first Shapiro step versus the phase difference β .

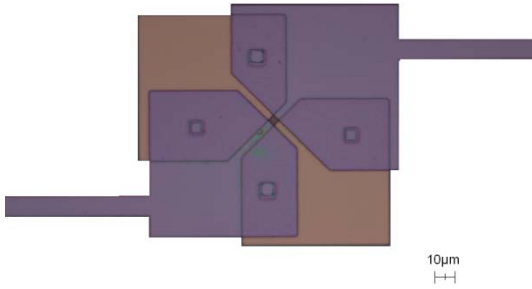
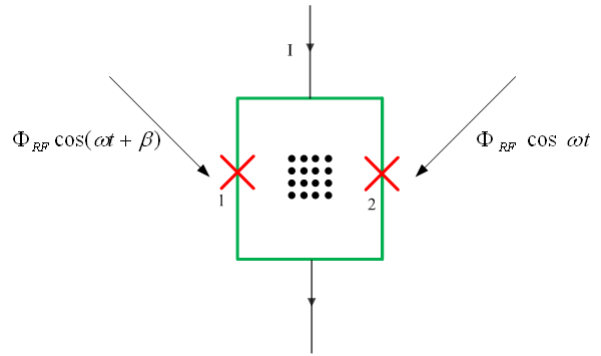


Figure 4. (a) The optical image of the one-cell SQUID circuit with two JJs.



(b) The sketch of the one-cell SQUID circuit. The JJs are indicated by the cross.

2.2.2 One-cell SQUID circuit with two JJs

Figure 4(a) shows the photograph of a one-cell SQUID circuit with two JJs. The dimension of the hole in the middle of the circuit is $4 \times 4 \mu\text{m}^2$. Figure 4(b) shows the sketch of the one-cell SQUID circuit. Two microwave signals are coupled to the

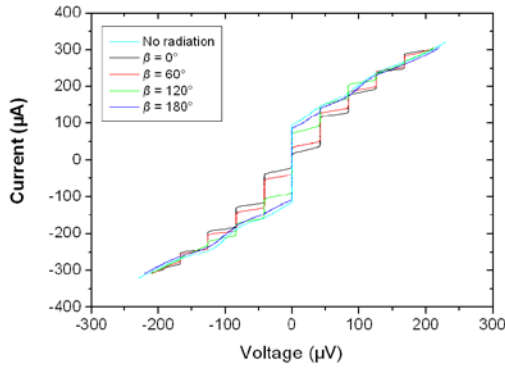
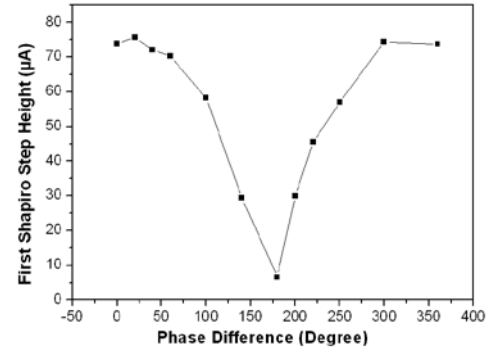


Figure 5. (a) The current-voltage characteristics of the one-cell SQUID for several different values of the phase difference β . The frequency of the microwave radiation is 20GHz.



(b) The dependence of the height of the first Shapiro step of the one-cell SQUID on the phase difference of two microwave radiation signals.

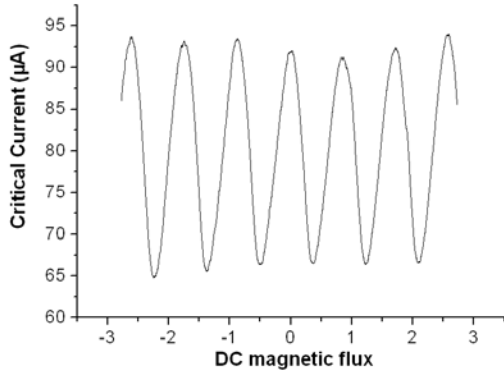


Figure 6. The dependence of the critical currents of the one-cell SQUID on the externally applied dc magnetic fluxes.

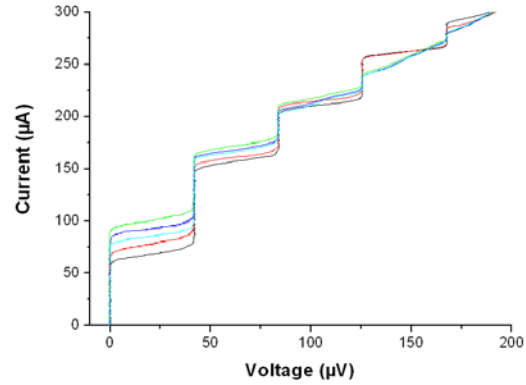


Figure 7. The current-voltage characteristics of one-cell SQUID under a microwave radiation. Different curves represent the current-voltage characteristics at different amplitudes of external dc magnetic fluxes.

circuit by two closely positioned coupling loops. The external applied dc magnetic field was induced by a coil placed underneath the circuit and was perpendicular to the plane of the substrate. The junctions are indicated by crosses in Figure 4(b).

The dependence of the current-voltage characteristics of the one-cell SQUID on the phase difference of two microwave radiation signals was investigated, which is shown in Figure 5(a). Figure 5(b) demonstrates the dependence of the current amplitude of the first Shapiro step of the one-cell SQUID on the phase difference between two microwave radiation signals. Comparing Figures 3(a), 3(b), and 5(a), 5(b) one can see that some characteristics of the one-cell SQUID under the radiation of two microwave signals are similar to those of the one-JJ circuit. We also observed here that the amplitude of the first Shapiro step varies with the phase difference β proportionally to $|\cos(\beta/2)|$. Furthermore, the maximum amplitude of the first Shapiro step is observed at $\beta = 0^\circ$ and the minimum height of the first Shapiro step is observed at $\beta = 180^\circ$. However, there is a difference between the SQUID and

single-JJ circuit. The critical current and the height of the Shapiro step of the one-cell SQUID can be adjusted in easy way by applying the external dc magnetic flux. Figure 6 shows the critical current of the one-cell SQUID as a function of external dc magnetic flux. Figure 7 illustrates the dependence of the Shapiro steps on the external dc magnetic flux under fixed microwave radiation power. The frequency of radiation microwave is 20 GHz.

2.2.3 Two-Cell SQUID with Seven JJs

Figure 8 shows the optical image of the two-cell SQUID circuit with seven JJs and the sketch of the geometry of the circuit. The dimensions of the holes in this circuit that we had available from previous experiments is $18 \times 18 \mu\text{m}^2$. The distance between the two holes is about $90 \mu\text{m}$. Two microwave radiation signals are coupled to the circuit by two closed coupling loops, which are as before placed above the sample. The external applied dc magnetic flux is induced by a coil located under the circuit.

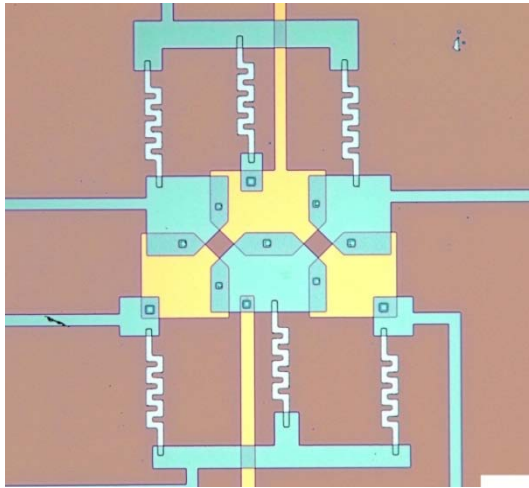
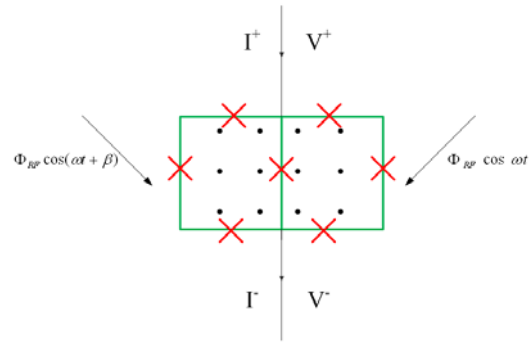


Figure 8. (a) Optical image of the two-cell SQUID with seven JJs. The dimension of the holes is $18 \times 18 \mu\text{m}^2$. The

distance between the two holes is $\sim 90 \mu\text{m}$.



(b) The sketch of the two-cell SQUID circuit. The seven JJs are indicated by crosses.

The magnetic field is perpendicular to the circuit plane and makes the magnetic flux in the two cells symmetric. Figure 9 illustrates the IV curve of the two-cell SQUID with (black line) and without (red line) microwave radiation. The frequency of the microwave radiation signal is 19.22 GHz. Under the chosen measurement temperature, the circuit has the critical current $I_c = 19 \mu\text{A}$, the normal resistance $R_n = 3.8 \Omega$, and the resulting characteristic frequency $f_c = 35 \text{ GHz}$. Figure 10 shows the critical current of the two-cell SQUID as a function of externally applied dc magnetic flux with no microwave radiation applied.

Figure 11 presents the current-voltage characteristics of two-cell SQUID irradiated by microwaves. Different curves represent the current-voltage characteristics with

different amplitudes of the external dc magnetic fluxes. The frequency of the microwave radiation signal is 19.22 GHz. It is evident that the characteristics of the Shapiro steps of the two-cell SQUID circuit are affected by the dc magnetic

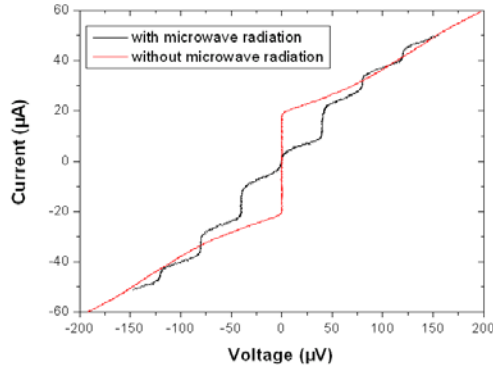


Figure 9. The current-voltage characteristics of two cell SQUID with (black line) and without (red line) microwave radiation. The frequency of the microwave radiation is 19.22GHz.

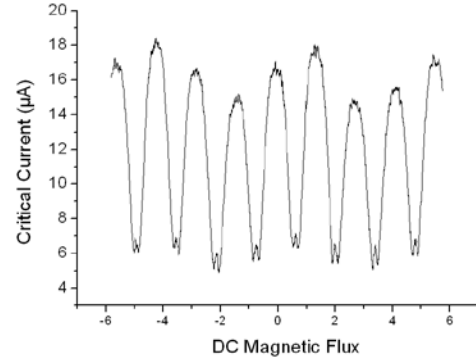


Figure 10. The dependence of the critical currents of the two-cell SQUID on the externally applied DC magnetic flux.

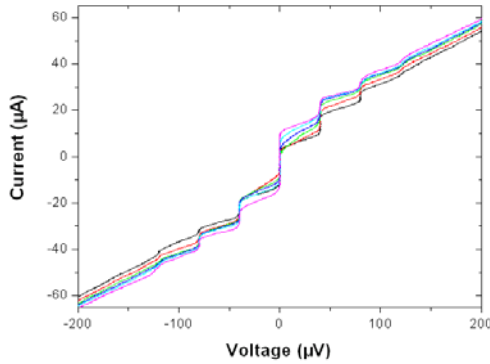


Figure 11. The current-voltage characteristics of the two-cell SQUID irradiated by a microwave signal. Different curves represent the current-voltage characteristics at different amplitudes of external DC magnetic fluxes. The frequency of the microwave radiation signal is 19.22GHz.

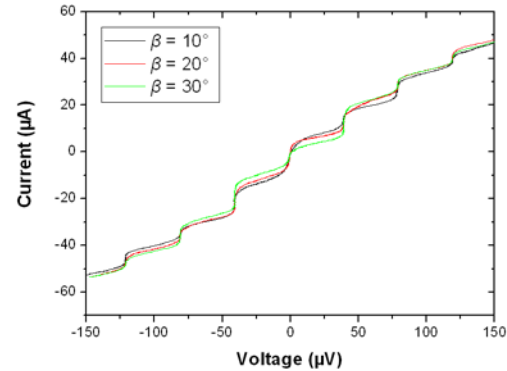


Figure 12. The current-voltage characteristics of the two-cell SQUID under the radiation of two microwave signals for different values of the phase differences β . The frequency of the microwave radiation is 19.22GHz.

flux. The experiments also demonstrate that the characteristics of the Shapiro steps can be influenced by the phase difference of the two microwave radiation signals. Figure 12 shows the current-voltage characteristics for phase differences of $\beta = 10^\circ$, $\beta = 20^\circ$ and $\beta = 30^\circ$. We can see from this figure that there are significant differences between these current-voltage characteristics.

To summarize, the characteristics of Shapiro steps vary as the phase difference β between two microwave signals changes. Therefore, one can record the voltage variation of the two-cell SQUID circuit by imposing a bias current on certain point

between e.g. the first Shapiro step and the zero-th Shapiro step (superconducting state). As demonstrated in Figure 13(a), when the bias current is set to the working point **a**, a variation of the phase difference produces a variation of the voltage from point **a** to point **b**. Figure 13(b) shows the dependence of the variation of the voltage on the phase difference. From this figure, we can see that there is $\sim 1 \mu\text{V}$ dc voltage variation induced

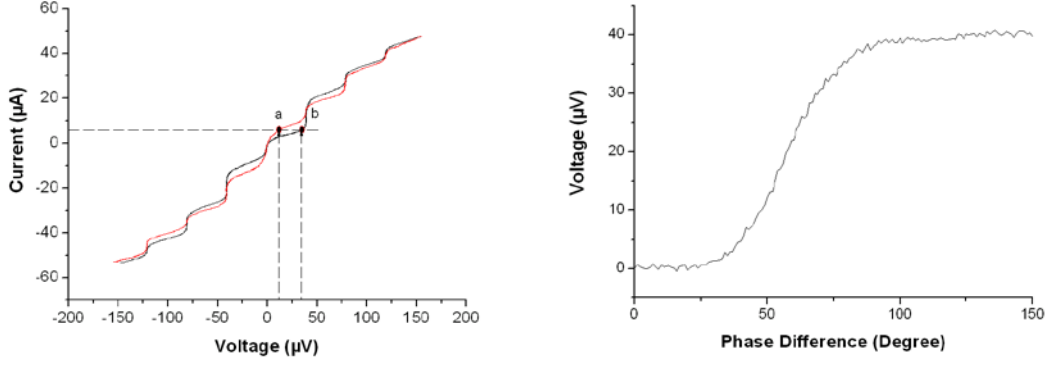


Figure 13. (a) The sketch of how to measure the voltage variations versus the phase difference. (b) The voltage variations versus the phase difference. The frequency of the microwave radiation is 19.22 GHz per degree near the steepest part of the curve, which means

$$\frac{\Delta V}{\Delta \beta} = \frac{1 \mu\text{V}}{\text{degree}}$$

We elaborate the phase difference issue a bit further in Figure 14. By considering the cells placed in free space, the phase difference β between the signals received by the two cells can be represented as:

$$\beta = \frac{2\pi d \sin \theta}{\lambda}$$

where θ denotes the angle of the incoming signal, d is the distance between two cells of the SQUID and λ is the wavelength of the incoming microwave radiation. In our experiments, the frequency of the incoming microwave signal is 19.22 GHz and $d = 90 \mu\text{m}$. As a result, when the incoming angle θ varies by 90° , the phase difference will

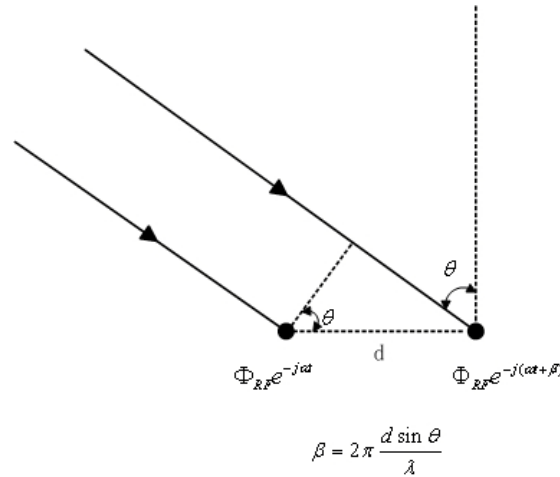


Figure 14. Schematic diagram of the relationship of incoming angle θ and the phase difference β .

vary $\sim 2.1^\circ$. Therefore, the voltage change becomes $\sim 0.02 \mu\text{V}$ for the incoming angle θ variation of 1° , which can be presented as

$$\frac{\Delta V}{\Delta \theta} = \frac{\Delta V}{\Delta \beta} \frac{2.1^\circ}{90^\circ} = \frac{20 \text{ nV}}{\text{degree}}$$

As we anticipate to show later, when adjusting the external dc magnetic fluxes through the two cells of the circuit to be antisymmetric or even asymmetric, the voltage change should be more sensitive to the phase difference of the microwave radiation signals.

3. New Design

Based on the experiment results, the new designs of the two-cell SQUID circuit with a phase shifter have been designed and have been submitted to the company of Hypres Inc. to be fabricated. Unfortunately, our initial submission to Hypres scheduled for June 2009 was delayed from the Hypres side till August and the samples have not been delivered until now. The delay with delivering the ordered samples made it impossible for us to present any new data for specially designed sample in this report.

Figure 15 shows the sketch and the layout of the two-cell SQUID circuit that we have designed and submitted to Hypres. In this circuit, we would like to impose a uniform symmetric external flux (the red control line at the bottom), for which the circulating currents tend to cancel out in the middle junction. Moreover, we also like to employ an asymmetric external flux so that half of the current is directed up on the left part of the SQUID and another half of the current is directed down on the right side (asymmetric flux is induced by the bottom black control line). This should lead to a much larger voltage change on the middle junction since the left and right hand side circulating currents should sum up in phase. Furthermore, we anticipate that the voltage signal of the middle junction can be boosted by a bifurcation when operating at an anti-resonance of the two cells. As the detection of both symmetric and anti-symmetric fluxes is necessary for the direction finding aspect to work, the voltages induced by symmetric external flux can be measured across the two junctions on the sides.

The directional coupling of the microwave field will be emulated by two synchronized microwave signals with tunable phase shifter. Two microwave signals will be individually coupled on-chip to the two SQUID cells. We also designed an on-chip tunable phase shifter made of another dc-SQUID circuit. By varying the bias current or dc magnetic flux of the SQUID, one should be able to adjust the inductance of the circuit and, at the same time, the phase of one of the microwave signals that comes through it [3].

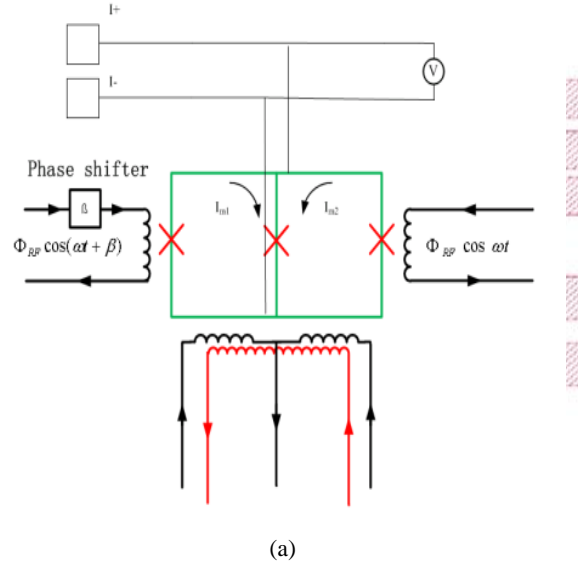


Figure 15. (a) The sketch and (b) the layout of the two-cell SQUID circuit.

4. Conclusion

We have reported preliminary experiments aimed at development of a sensitive microwave directional sensor based on a two-cell SQUID by imitating the operational principle of the fly's ears. Several available Josephson junction (JJ) and SQUID circuits have been measured. We have detected the response of two different SQUID circuits to small variations of the phase of two microwave signals that were coupled to the circuits. The resulting projected the dc voltage sensitivity has been estimated as $0.02 \mu\text{V}$ under the change of the phase difference of the microwave radiation signal of 1° . Furthermore, based on these experimental results we have designed specially tailored SQUID circuits with two on-chip microwave ports and a phase shifter, which have been submitted for fabrication to Hypres foundry.

References

- [1] R. N. Miles, D. Robert, and R. R. Hoy, Mechanically coupled ears for directional hearing in the parasitoid fly *Ormia ochracea*, *J. Acoust. Soc. Am.* **98**, 3059 (1995).
- [2] D. Robert, R. N. Miles, and R. R. Hoy. Tympanal mechanics in the parasitoid fly *Ormia ochracea*: intertympanal coupling during mechanical vibration. *J comp Physiol A* **183**, 443 (1998).
- [3] M. Sandberg, C. M. Wilson, F. Persson, T. Bauch, G. Johansson, V. Shumeiko, T. Duty, and P. Delsing, Tuning the field in a microwave resonator faster than the photon lifetime, *Appl. Phys. Lett.* **92**, 203501 (2008).